Stratigraphic differentiation for the recognition of geological units on single-channel seismic lines through the use of the 2D Fast Fourier Transform: an application example created in the Gulf of Naples

A. Giordano[1], L. De Luca[1], A. Gifuni[1], P. Giordano[2] and M. Prisco[3]

[1] University of Naples Parthenope, Naples, Italy
[2] JMA Wireless Italia Technology Center-Teko Telecom, Castel San Pietro Terme, Bologna, Italy
[3] University of Naples Federico II, Naples, Italy

ABSTRACT   The seismic-stratigraphic analysis of single-channel seismic profiles does not provide reliable information on the nature of the materials identified in the absence of direct investigations; therefore, it is often affected by interpretative subjectivity. In this work, we use the 2D Fast Fourier Transform, applied to samples extracted from areas of interest, as a method to obtain a database of signatures (characterisation indices) for post-processing identification of geological units. This method is applied to discriminate Holocene marine units from volcanoclastic units present in the geological records of the Gulf of Naples. The results show how the signatures of these units are specific and, consequently, can be well distinguished using the proposed method. The method is corroborated by the statistical analysis carried out on single shots extracted from the seismic lines. Although the proposed method may lead to misinterpretations in some specific cases, as discussed in the paper, it offers geologists important help in rapidly and effectively classifying seismic units.

1. Introduction

Reflection seismics is a geophysical investigation technique that exploits the elastic properties of the subsoil and enables the detection of characteristics and geometry of rock formations underlying the Earth's surface (marine subfloor) with high precision. It consists in the generation of pulses of short duration and limited amplitude using specific sources; the signals reflected from the seabed and from the various underlying thicknesses (seismic traces) are subsequently collected and recorded by special sensors (hydrophones) organised according to specific geometric configurations.

The set of all seismic traces, simultaneously recorded in response to each single energisation, forms a seismic recording (seismic line). The seismic line is a reproduction, in units of time, of a part of the interior of the marine subfloor along the route examined. It consists of a vertical stratigraphic model, which presents itself in the form of seismographic features with different shades of grey (McQuillin *et al*., 1979; Urick, 1979).

Along the horizontal plane of the seismic line, the various reflectors are the response caused by the variations in a different acoustic impedance, *Z*, at the separation surface between the

various layers (Jones, 1999; De Dominicis Rotondi, 1990). That is, each layer has its own acoustic behaviour, due to the different composite materials (density variation):

$$Z=\rho \cdot v \hspace{6cm} (1)$$

where ρ is the density of the materials and v the speed of sound in the materials.

The geological interpretation and seismic-stratigraphic analysis of these reflections does not provide certain information on the nature of the identified units. It is often characterised by interpretative subjectivity on the part of the geologist, in the absence of direct investigations.

In this work, a method is proposed to facilitate the geological interpretation of seismic profiles for the recognition and discrimination of seismic units. The procedure and related data processing, which will be presented in section 2, was developed in the Matlab environment (Math-Works) and incorporated into a self-built toolbox, herein called the Seismic CLASS toolbox. The main screen and block diagram of the toolbox are shown in Fig. 1.
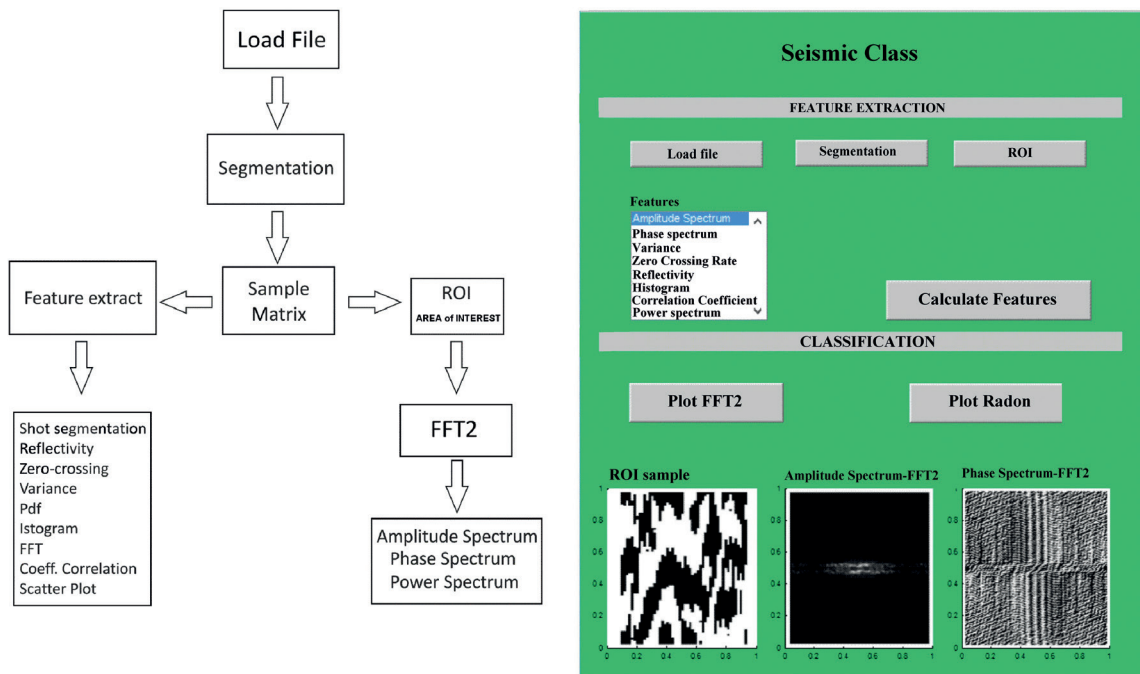
Fig. 1 - Main screen of the Seismic CLASS toolbox and relative block diagram.

The proposed method is tested on two known seismic units, present in the geological records of the Gulf of Naples. More specifically: 1) the Holocene marine unit, identified as unit D. 2) the volcanic clastic unit (Campanian ignimbrite), identified as unit IC. These units have been identified and confirmed over the years by various authors (Milia and Torrente, 1997, 1999, 2003; Milia *et al.*, 1998b; Mirabile *et al.*, 1998; Acocella and Funiciello, 1999, 2006; Aiello *et al.*, 2001, 2005, 2007; Acocella *et al.,* 2004), who progressively calibrated and correlated the stratigraphic data directly with the wells for geognostic investigations. The most important reference well for this validation is the Trecase1 well (Ippolito *et al.*, 1973; Rosi and Sbrana,

1987; Bellucci, 1998; Milia *et al*., 2003, 2011). It was drilled by AGIP (an Italian automotive gasoline and diesel retailer) and ENI (an Italian multinational energy company) between 1980 and 1981 and was first described by Brocchini *et al*. (2001). The well is located on the south-eastern slopes of the Vesuvius. Fig. 2 shows the stratigraphy of the well excavation. It should be noted that on the summit there are volcaniclastic deposits with the presence of a layer of approximately 30-35 m of Campanian pre-ignimbrite and a further layer of approximately 65 m of Campanian ignimbrite [270-116 kyr B.P. (Rolandi and Bellucci, 2003; Milia and Torrente, 2011) and 39 kyr B.P. (De Vivo *et al*., 2001)]. Therefore, these two identified and confirmed units are used as references to test the proposed model.
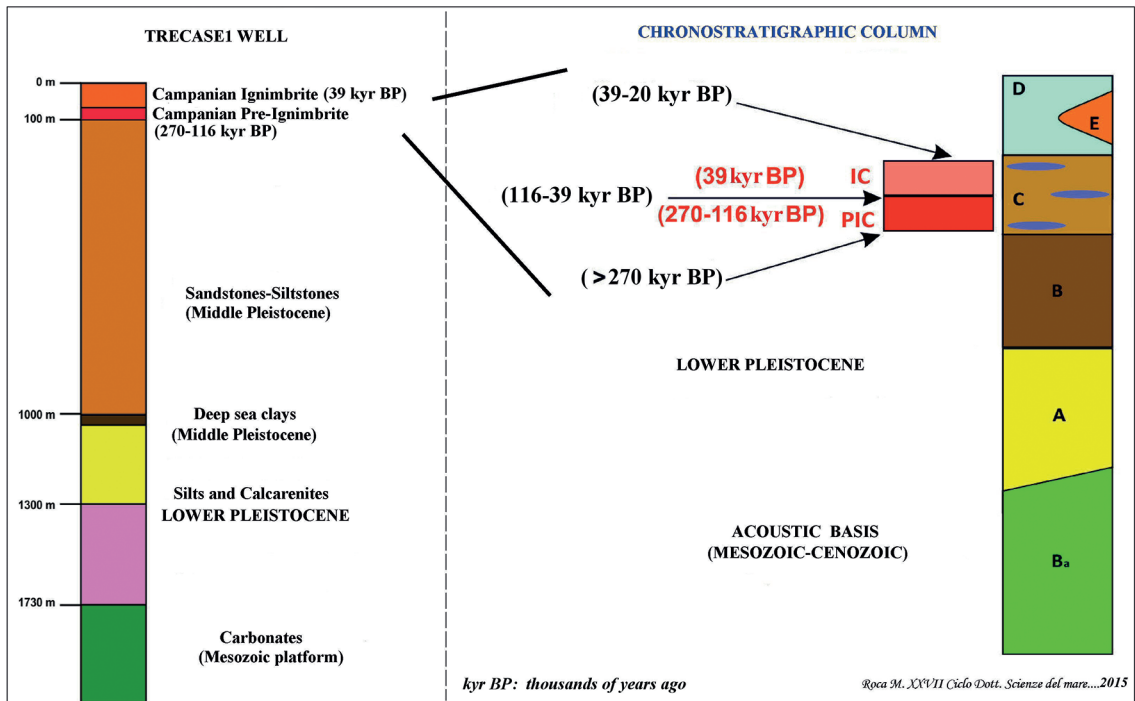
Fig. 2 - Stratigraphy of the Trecase1 well (Milia *et al*., 2003; Milia and Torrente, 2011).

For the tests carried out in this work, two seismic lines, acquired during the study of bradyseism in the Gulf of Naples and Gulf of Pozzuoli (1986-1990), were taken into consideration as they include the two geological units mentioned above, units D and IC (Milia, 1999; Milia and Torrente, 2003; D'Argenio *et al*., 2004; Roca, 2015). The two lines, called lines L3_90 and L5_90, are highlighted by bold green lines in the navigation plan (Fig. 3). It should be highlighted that the two lines were acquired from the same seismic source, i.e. the Multispot Extended Array Sparker, during the seismic campaign in the Gulf of Naples in 1990 (Mirabile *et al*., 1969, 1991, 2000; Buogo and Cannelli, 1999; Simpkin, 2005). These lines refer to the same depositional environment.

For the two seismic lines the following acquisition parameters were respected: sampling frequency of 12 kHz, distance between traces of 6 s, boat speed of 1.8 m/s and listening time of 1 s.

Fig. 3 - Navigation plan of the Gulf of Naples: the lines used are bold green.

2. Seismic CLASS: data processing and methods

Data processing is carried out with the Seismic CLASS toolbox mentioned above. From the reflectivity (*R*)[1] matrix of each of the two interpreted seismic lines (Milia *et al.*, 1998a, 2000; Milia and Torrente, 1999), through a simple segmentation process, which can be manual and/or automatic, the ROI[2] samples are extracted for both the IC units and for the D units, according to the block diagram in Fig. 1. For each ROI, the 2D spectrum is calculated using the 2D Fast Fourier Transform (FFT2) tool (Elias Fakiris *et al.*, 2012).

For the extraction of ROI samples, the seismic line was imported into the Seismic CLASS toolbox and the Imcrop and/or roipoly commands of MathWorks (https://www.mathworks.com/products/image-processing.html) were used (Figs.1 and 4).

Imcrop returns the cropped part of an image (ROI). It is converted into a binary image called a target image, and, then, sent to the FFT2 calculation toolbox for further processing. Therefore, both the 2D amplitude spectrum and the phase spectrum are calculated for each ROI.

The Crop Image tool is a movable, resizable rectangle that can be interactively positioned

---

[1] *R* is intended as the amount of energy (absolute value), contained in the single segment.
[2] ROI = Region of interest or extracted sample.

Fig. 4 - Flow diagram of the processing phases.

over areas of interest using the mouse. The crop rectangle is located and cut by clicking and dragging with the mouse.

Initially the samples are manually extracted, with ROI matrices of 90×50 elements. This choice is linked to the minimum thickness identified on the seismic lines during the interpretation phase. Once extracted, the samples are sent to the FFT2 of the Seismic Class toolbox, according to the flow diagram in Figs. 1 and 4.

The interpreted seismic lines are shown in Fig. 5, whose caption specifies, for completeness, the other seismic units identified during the interpretation (see stratigraphy in Fig. 2). An example of some samples taken from the seismic lines are shown in Fig. 6. Clearly, the choice of ROI, as previously mentioned, depends on the thickness, under examination, identified on the interpreted seismic lines.

2.1. Results

This section reports the results of the methodology applied to the two seismic lines examined.

Figs. 7 and 8 show examples of responses of the ROI samples (units IC and D) extracted from the two seismic lines, as well as the related 2D amplitude and phase spectra. We note that both unit D and unit IC present a distinctly different signature as they depend on the different sedimentological contents. In fact, by analysing the two ROIs, the image of the IC unit sample is noted to be rather chaotic, unlike the D unit sample, which shows a smooth and uniform appearance along the horizontal plane, similarly to the reflectors on the interpreted lines.

Fig. 9 shows the amplitude spectrum of the D and IC units of line L5_90; in particular, these images show a 3D representation (profile view) of the power spectrum.

In Fig. 10, the responses of the two units are compared in terms of power spectrum. To do so, they have been slightly tilted for better visualisation/interpretation. A clear difference between the two responses is noted.
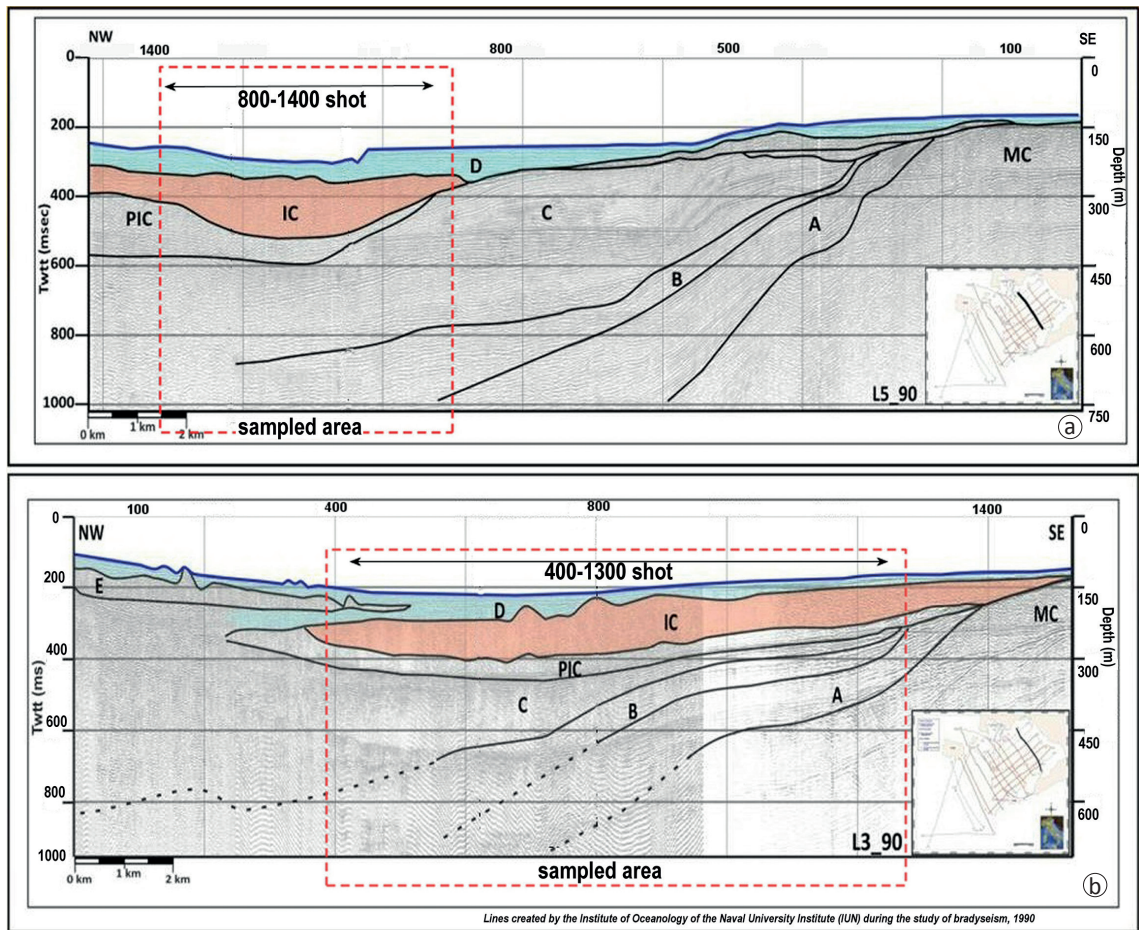
Fig. 5 - Seismic line interpretation: a) L5_90, b) L3_90. D unit = upper Pleistocene-Holocene marine sediments (39 kyr BP); IC unit = Campanian ignimbrite (39 kyr B.P.); PIC unit = pre-Campanian ignimbrite tuffs (270-116 kyr B.P.); C unit = middle-upper Pleistocene marine sediments; B unit = lower-middle Pleistocene marine sediments; A unit = upper Pliocene-lower Pleistocene marine sediments; MC unit = meso-Cenozoic carbonate bedrock (acoustic basement).

Fig. 11 compares the responses of the amplitude spectrum of additional ROI samples taken from lines L3_90 and L5_90 both for unit D and unit IC. A clear spectral difference is noted again.

Fig. 12 shows images from additional samples taken from the two seismic lines; these images and relative information can be noted to be consistent with previous results.

2.2. Discussion

The low frequencies are distributed in the centre of the image produced by the FFT2 (amplitude spectrum), while the high frequencies are distributed on the sides of the image itself.

From the results of Fig. 7 (unit IC), almost all the spectral power can be noted to be concentrated in the centre of the image and is characterised by low frequencies [Fig. 7b (Oliva *et al.*, 1999; Oliva and Torralba, 2001, 2002; Torralba and Oliva, 2003)], while in Fig. 8 the amplitude spectrum of unit D visually shows a double structure along the horizontal plane, characterised by a distribution oriented towards high frequencies (Fig. 8b).
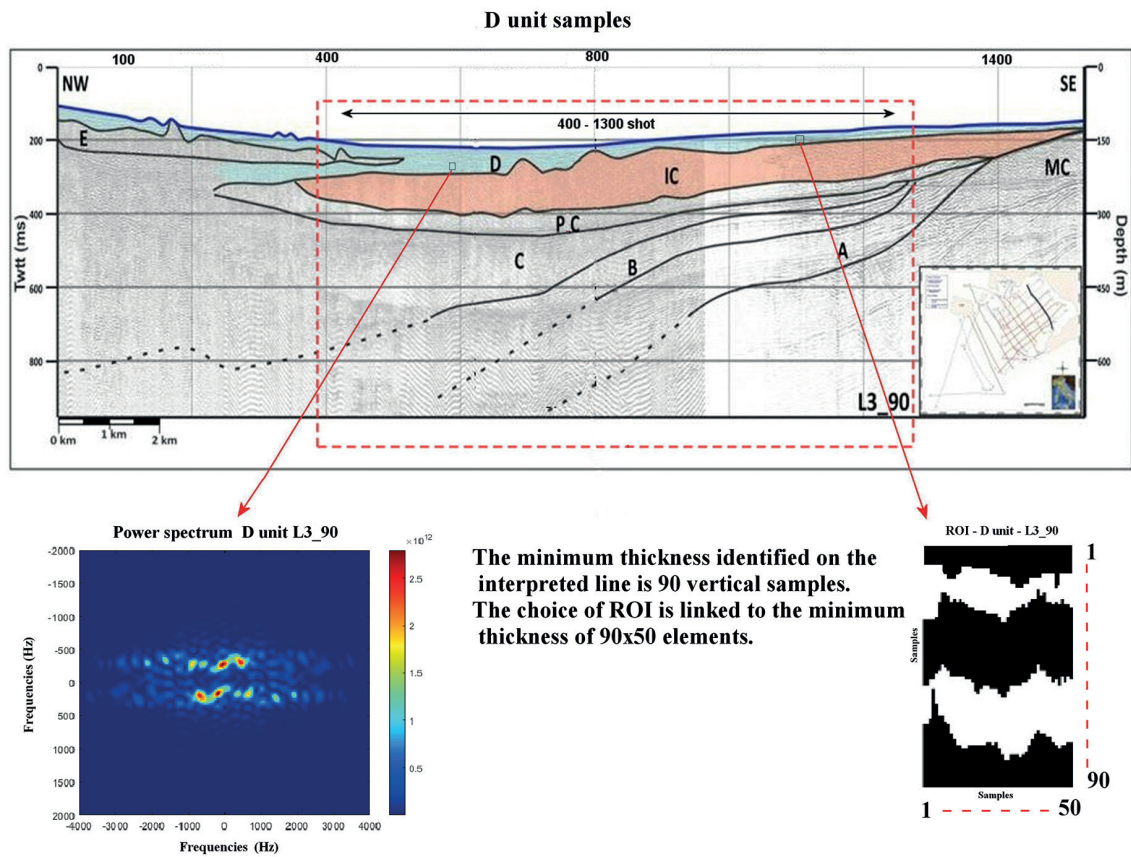
Fig. 6 - Example of samples taken from the seismic lines.

Since the D unit is the first layer on the seismic lines, it is characterised by high frequencies, as expected, while the IC unit, located below the D unit, is cleared of high frequencies, with a tendency towards low frequencies. The signatures of the two units are very distinct: unit IC appears quite homogeneous and chaotic, while unit D is quite linear with stratifications as they appear on seismic lines.

Since the results of the proposed method not only depend on the propagation characteristics of the materials and its discontinuities but also on the structural geometry of the material, it must be considered that, in cases of inversions or bendings of the reflectors, we are faced with an ambiguous situation in the relative responses. In these cases, the proposed method should not be applied to avoid misinterpretations. In fact, Figs. 9 and 10 confirm this in the 3D representation, displaying a profile of the response of the 2D power spectrum.

In the next section, cross correlation will be used to statistically compare the two responses.

3. Corroborations of the method: estimation of statistical parameters of seismic signals

In this section, the proposed method is confirmed by applying statistical analyses.

Using the additional tools contained in the Seismic CLASS toolbox, a series of equidistant
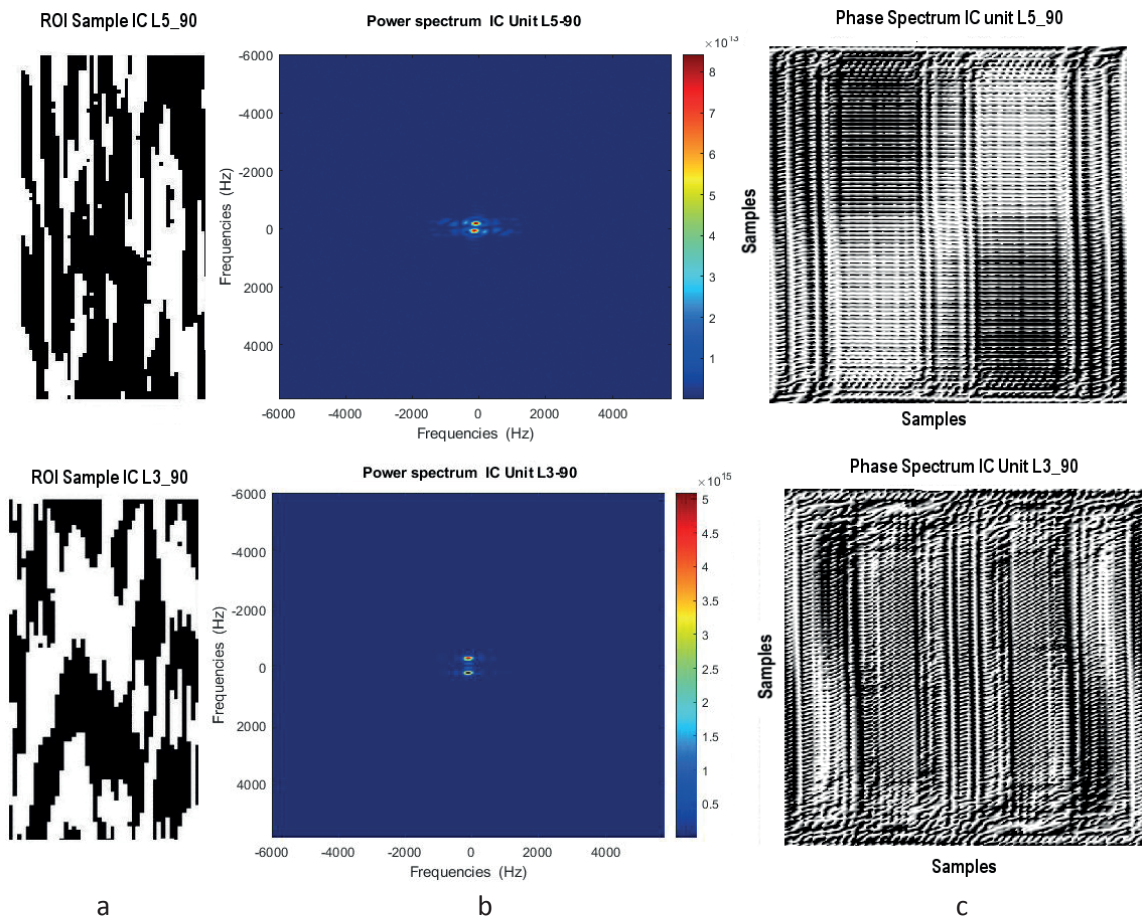
Fig. 7 - IC unit (L5_90 line-L3_90 line): a) ROI sample; b) amplitude spectrum response, FFT2.; c) phase spectrum response.

shots (for a total of 15 shots) were extracted from the two interpreted seismic lines, within the chosen intervals (Table 1) in order to cover and characterise the entire area of interest (hatched area on the lines indicated in Fig. 5), both for the IC unit and D unit. An example of the extracted shots is shown in Fig. 13, where they are expressed in the time domain.

A segmentation process is, then, applied to the extracted shots (Giordano and Giordano, 2012; Giordano *et al.*, 2015). Fig. 14 tries to explain the methodology applied to extract the various shots from the lines. With the help of the interpretation made on the two lines (Fig. 5), the segmentation process is applied to the shots. With this procedure, portions of the signal, corresponding to the thicknesses identified on the seismic lines, are obtained. Fig. 15 shows some segments of the IC unit, extracted from the shots.

Table 1 - Chosen intervals of the sampled area to characterise the object units.

Line	Shots-range
L5_90	800÷1400
L3_90	400÷1300
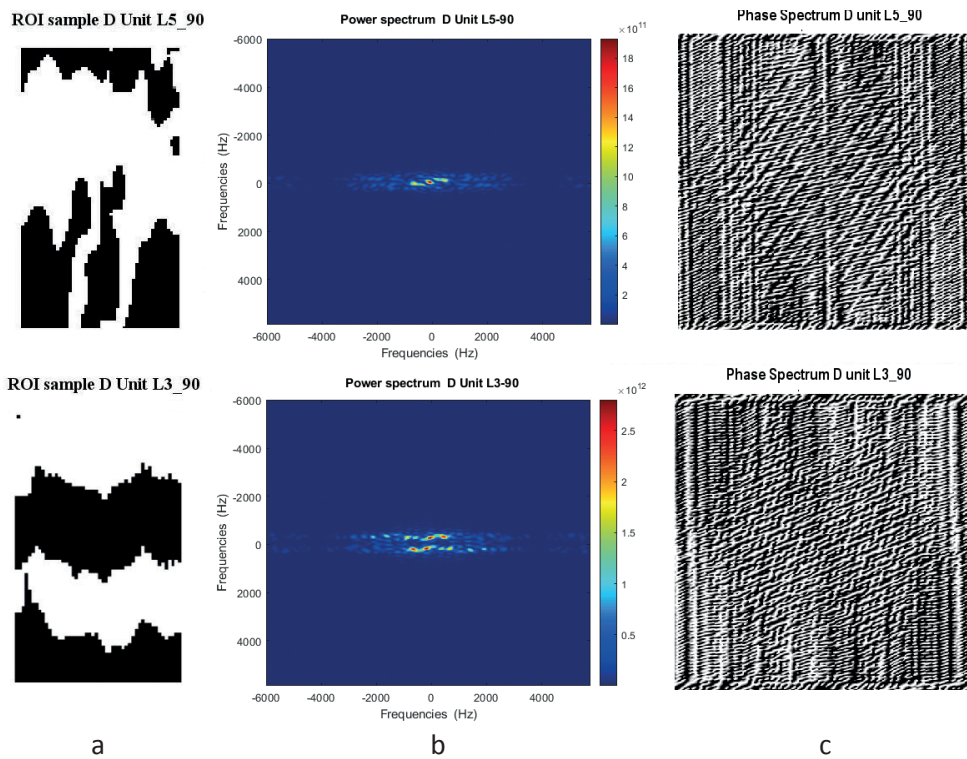
Fig. 8 - D unit (upper panel L5_90 line, lower panel L3_90 line): a) ROI sample; b) amplitude spectrum response, FFT2; c) phase spectrum response.
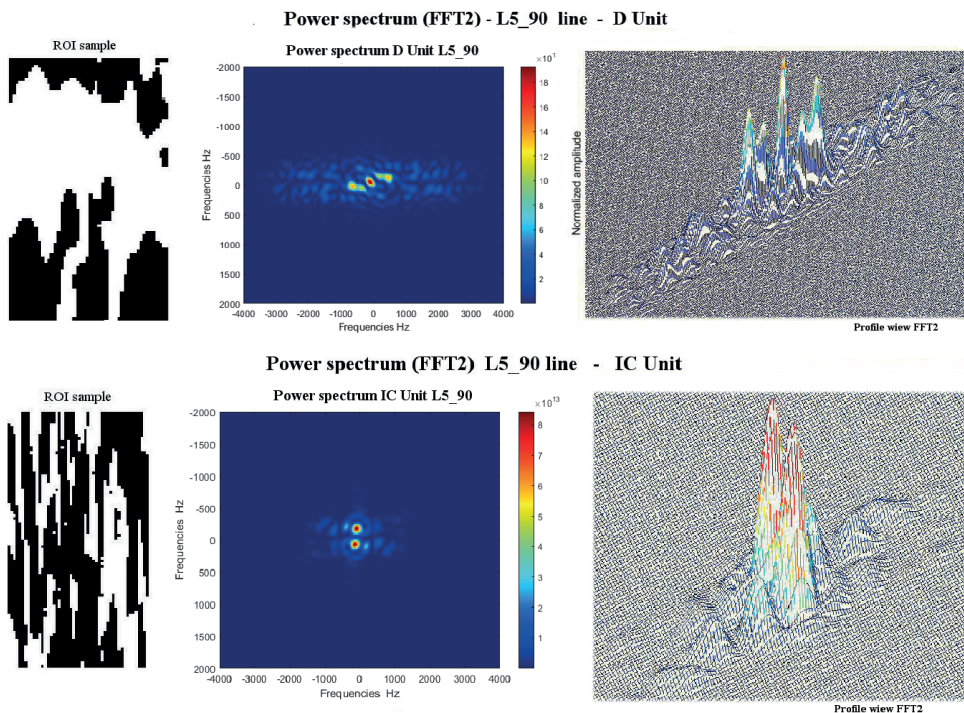
Fig. 9 - Picture sample and relative amplitude spectrum, line L5_90: a) D unit; b) IC unit.
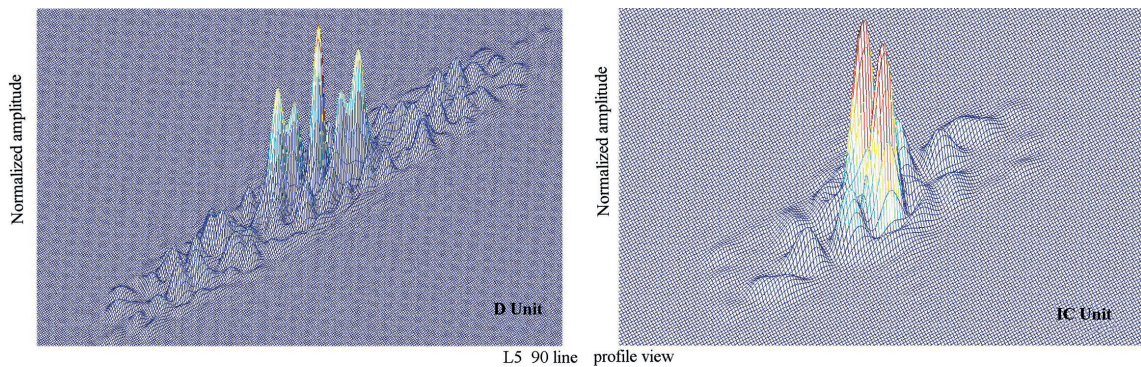
Fig. 10 - Comparison of the amplitude spectrum of the D unit and IC unit, L5_90 line (the spectra are slightly tilted for better viewing).

For each segment, statistical analyses are performed, including: zero-crossing index, variance, *R*, distribution and relevant histogram, 1D amplitude spectrum (FFT). Ultimately, the responses obtained are compared, by calculating the correlation coefficient and the scatter plot between the various units, for the same line and between different lines.

3.1. Statistical analysis

Table 2 shows the values of the zero-crossing and variance indices, of the IC and D units, from the segments extracted from the various shots. The comparison of the data relating to the IC unit and D unit, taken from the two seismic lines, has provided a remarkable result, in particular for the statistical index variance.

For the IC unit, the variance occurs, on average, with very low values compared to the results obtained for the D unit, highlighted in red in Table 2. Although the response of the zero-crossing index is unsatisfactory as it is linked to the length of the extracted signal (it coincides with the identified thickness), it should, however, still be taken into consideration. The zero-crossing index referring to the D unit presents slightly lower values compared to the IC unit. The IC unit appears inhomogeneous (non-uniform), as per the response on the seismic line. Furthermore, the D unit, characterised by decidedly high variance values compared to the values of the IC unit, highlights an important characteristic for materials whose nature presents variable and non-homogeneous traits.

Fig. 16 confirms the results obtained in Table 2, showing the data distribution trend and histograms, related to the IC units and D units, for the two sample lines examined.

Unit D shows a flattened histogram on the ordinate axis with high variance values, while unit IC shows a sharp histogram on the ordinate axis with low variance values. We can, therefore, state that the histogram relating to the IC unit, of L5_90 and L3_90, presents a distribution whose trend is unimodal and characterised by a low variance value, while the histogram representing the D unit presents a distribution with a bimodal trend with a high variance value, as shown in Table 2. Ultimately, it can be said that unit D is characterised by a thickness whose *R* matrix is non-homogeneous, with traits of variability throughout the entire unit, while unit IC, conversely, is characterised by low variability, resulting in a thickness whose *R* matrix is almost homogeneous to the eye, according to the ROI samples (Figs. 7 and 8).

Table 3 shows the results obtained from the distributions of Fig. 16. At a first analysis, the variance values determined by the individual thicknesses of Table 2 are found to be 100%
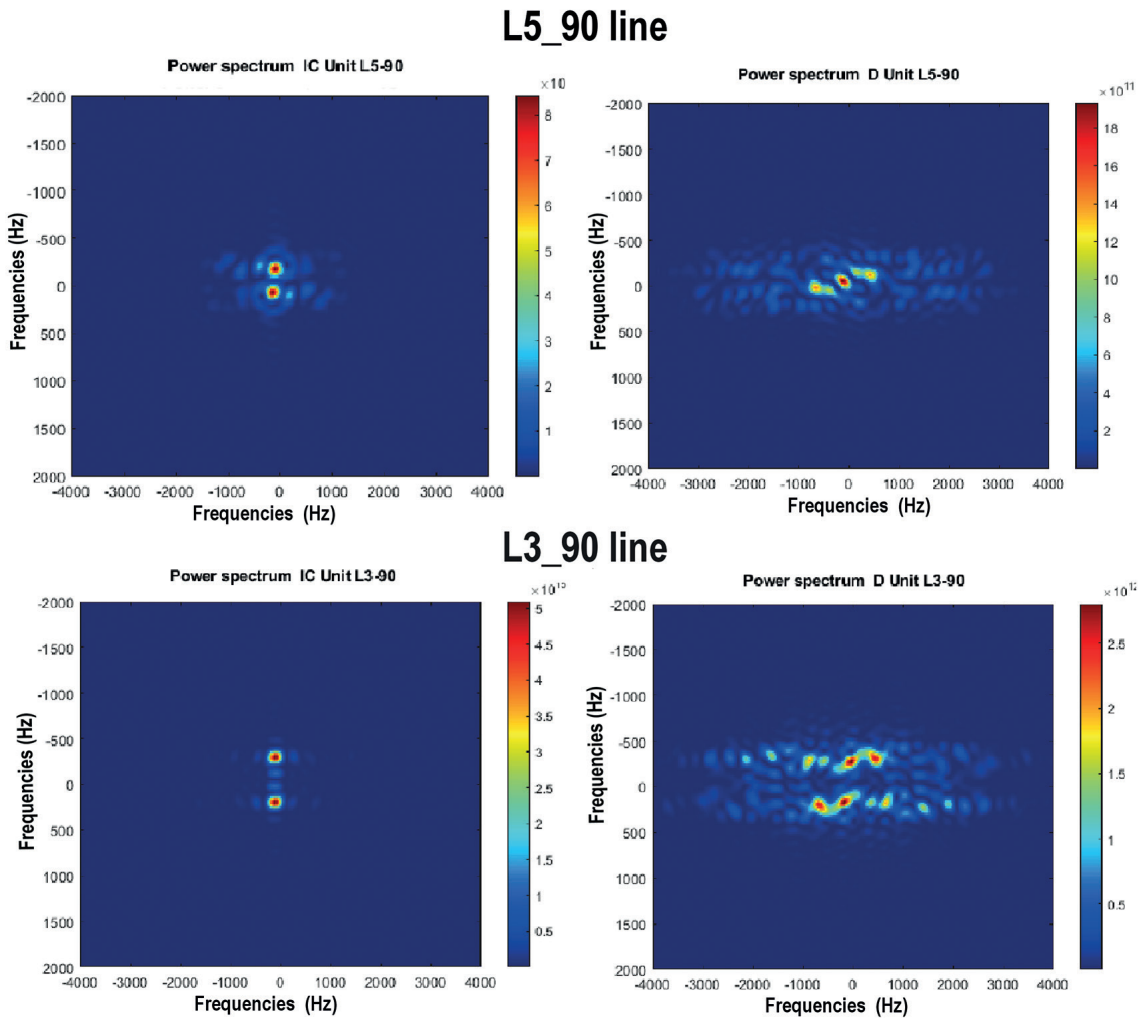
Fig. 11- Power spectrum: comparison between unit IC and unit D. Images are slightly zoomed for better reading.

comparable with these responses, certainly proving that the IC unit is characterised by a low variance, while the D unit is characterised by high variance values.

R is a very significant index; it characterises the materials by highlighting the hardness and compactness of the thickness in question. Table 4 shows the *R* indexes of the IC units and D units relative to the signals (thicknesses) extracted from the indicated shots. It can be noted that *R* of the IC unit presents much higher values than that of the D unit, a characteristic of compact and fairly hard materials compared to the surface sediments of the Holocene (D unit).

4. FFT spectral analysis: result comparisons

For the decoding of the information contained in our signals, the 1D FFT implemented in the Seismic CLASS toolbox is applied as a tool. Its objective is to evaluate the weight of the various frequency components on the signal (thickness) under examination.
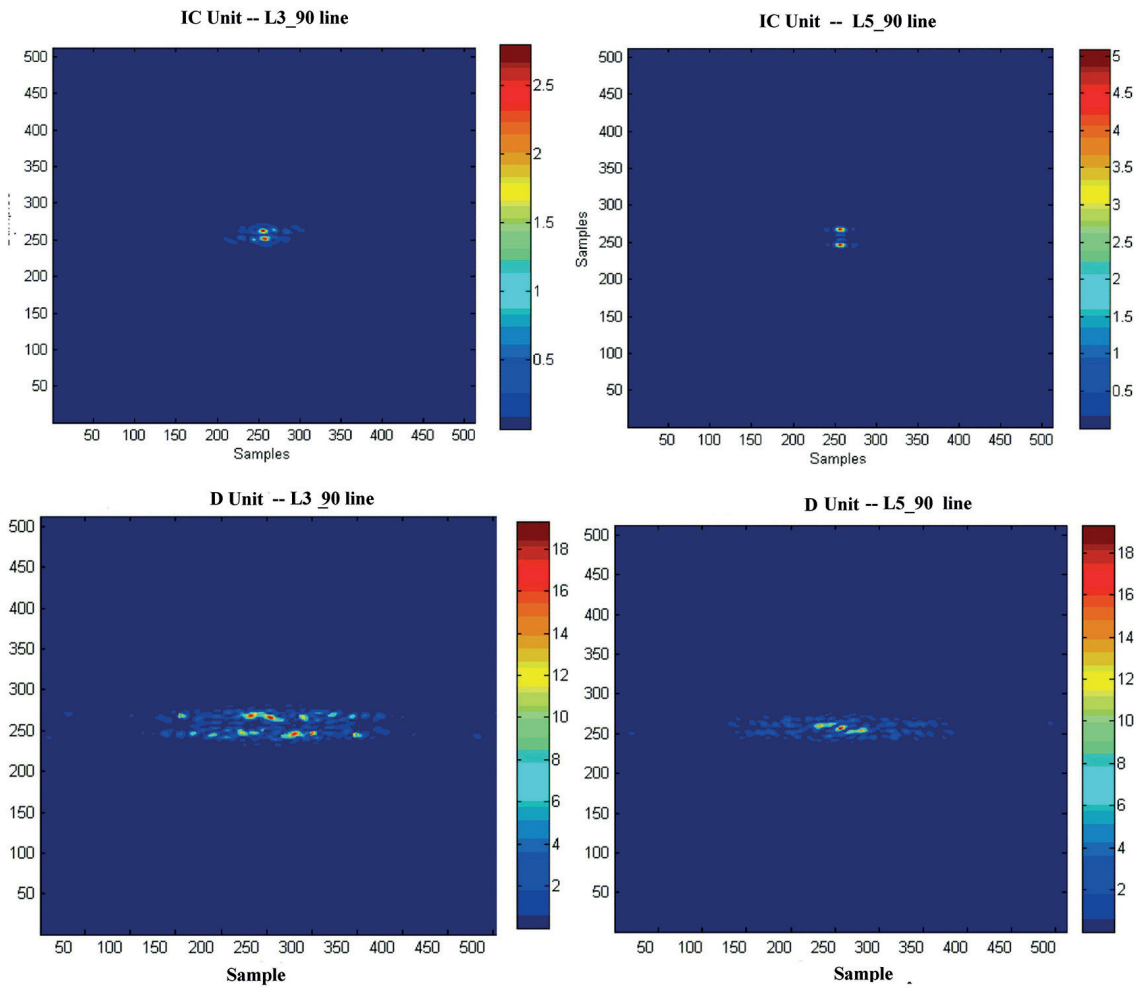
Fig. 12 - Additional samples taken from the seismic lines for the two IC (upper panel) and D (lower panel) units, the axes are expressed in samples.
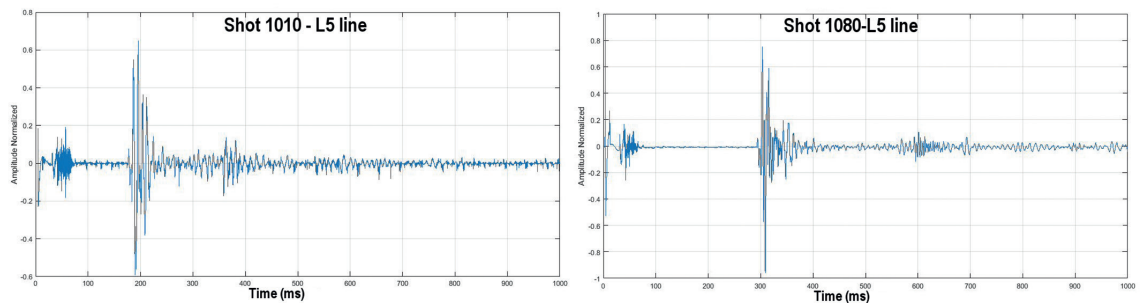
Fig. 13 - Example of shots extracted from lines.
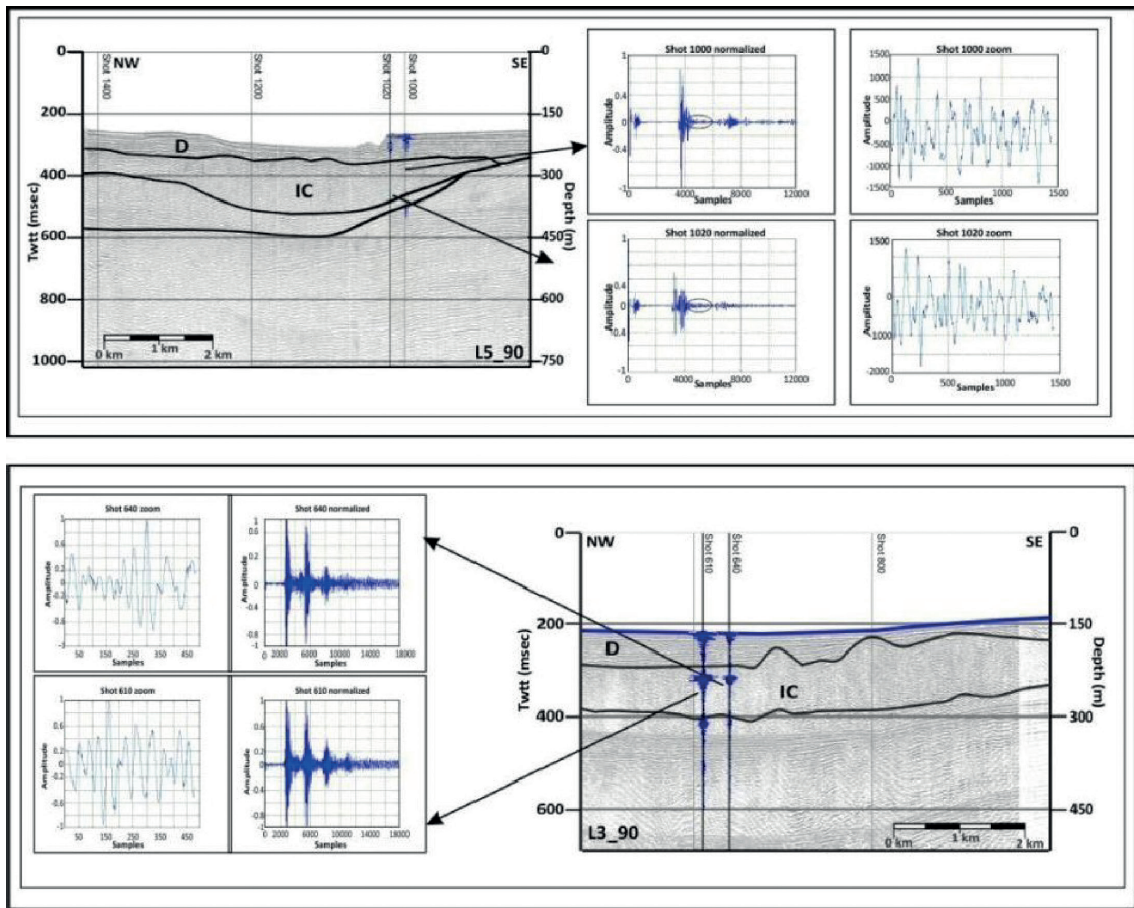
Fig. 14 - Segments extracted from seismic lines.
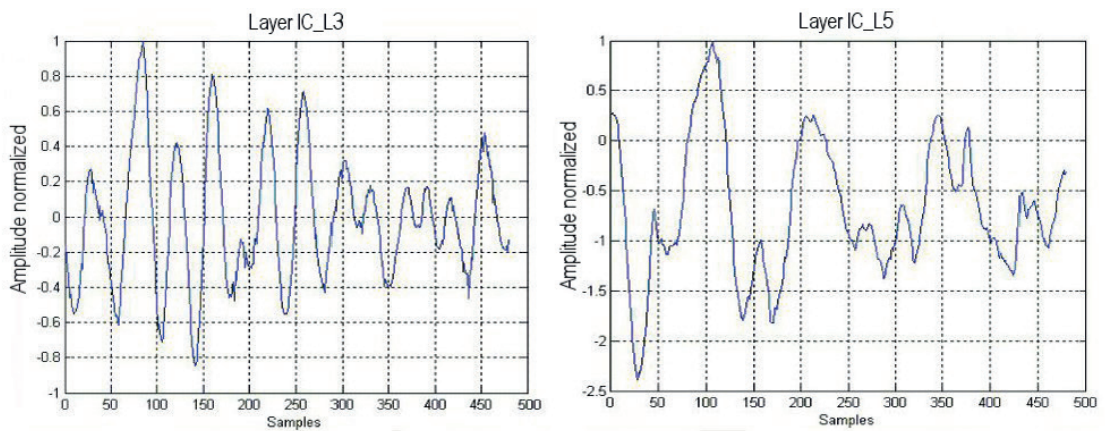
Fig. 15 - Example of extracted segments.
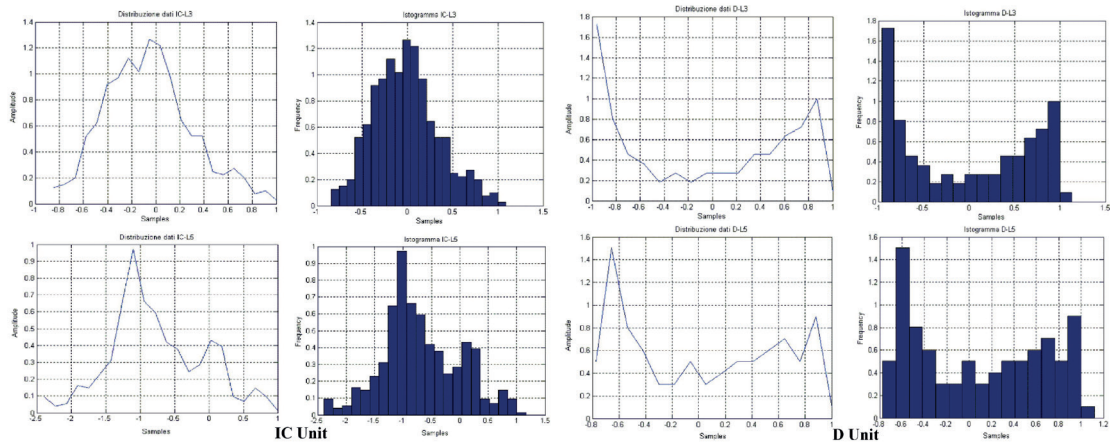
Fig. 16 - Data distribution charts relative to the IC layer histograms and D layers.

L5 90-D Unit		
Shot	**Zero-crossing**	**Variance**
800	36	0.1826
840	35	0.0976
880	35	0.1988
920	36	0.1119
960	33	0.2621
1000	36	0.1142
1040	33	0.3044
1080	37	0.0709
1120	35	0.1431
1160	41	0.1253
1200	36	0.1074
1240	34	0.2657
1280	45	0.1318
1320	38	0.1163
1360	35	0.0946
	Zero-crossing mean	**Variance mean**
	36.33333333	**0.155**

L3 90-D Unit		
Shot	**Zero-crossing**	**Variance**
450	54	0.2079
490	56	0.1632
530	49	0.1915
570	39	0.2300
610	44	0.2105
650	37	0.2238
690	44	0.1349
730	37	0.1972
770	32	0.1226
810	26	0.1523
850	30	0.1582
890	12	0.0664
930	13	0.0714
970	24	0.1156
1010	16	0.1395
	Zero-crossing mean	**Variance mean**
	34.2	**0.159**

L5 90-IC Unit		
Shot	**Zero-crossing**	**Variance**
800	32	0.0423
840	67	0.0859
880	24	0.0370
920	22	0.0798
960	73	0.0860
1000	31	0.0680
1040	36	0.1159
1080	53	0.0711
1120	36	0.0940
1160	28	0.1103
1200	38	0.0682
1240	40	0.1038
1280	69	0.0611
1320	32	0.0526
1360	51	0.0010
	Zero-crossing mean	**Variance mean**
	42.13	**0.072**

L3 90-IC Unit		
Shot	**Zero-crossing**	**Variance**
450	90	0.0111
490	79	0.0103
530	76	0.0090
570	90	0.0085
610	75	0.0114
650	80	0.0066
690	77	0.0076
730	76	0.0334
770	89	0.0301
810	81	0.0470
850	79	0.0142
890	59	0.0021
930	65	0.0011
970	33	0.0127
1010	15	0.0875
	Zero-crossing mean	**Variance mean**
	70.9	**0.020**

Table 2 - The table shows the zero-crossing and variance values of the segments extracted from the shots obtained from the two seismic lines. The values of unit D are represented in the upper row and those of unit IC in the lower row. The values show a clear difference: unit D is characterised by high variance, while unit IC by low variance.

Table 3 - Response relating to the data distributions in Fig. 15.

	IC-L3_90	IC-L5_90		D-L3_90	D-L5_90	
Variance	0.02	0.072		0.159	0.155	
Mean	-0.02	-0.40		-0.02	-0.21	
Median	-0.027	-0.795		-0.018	-0.556	

Table 4 - *R* of some thicknesses extracted from the relative shots.

Shot – L5_90	920	960	1000	1040	1080	1160
R D unit	14.79	19.39	17.29	23.76	23.32	14.58
R IC unit	7.26	7.33	9.59	8.55	6.72	6.61
Shot – L3_90	570	610	650	690	730	810
R D unit	14.75	19.39	74.29	43.76	23.28	13.59
R IC unit	8.67	7.52	6.23	7.26	7.33	9.59

Fig. 17 presents some results obtained for the two geological units under examination. Data processing shows that the IC unit is oriented towards low frequencies, in particular, it is involved in a range of frequencies that vary in band (from 200 to 500 Hz). Unit D is characterised by much higher frequencies, reaching components around 2,000 Hz, as can be seen from the images in the figure.
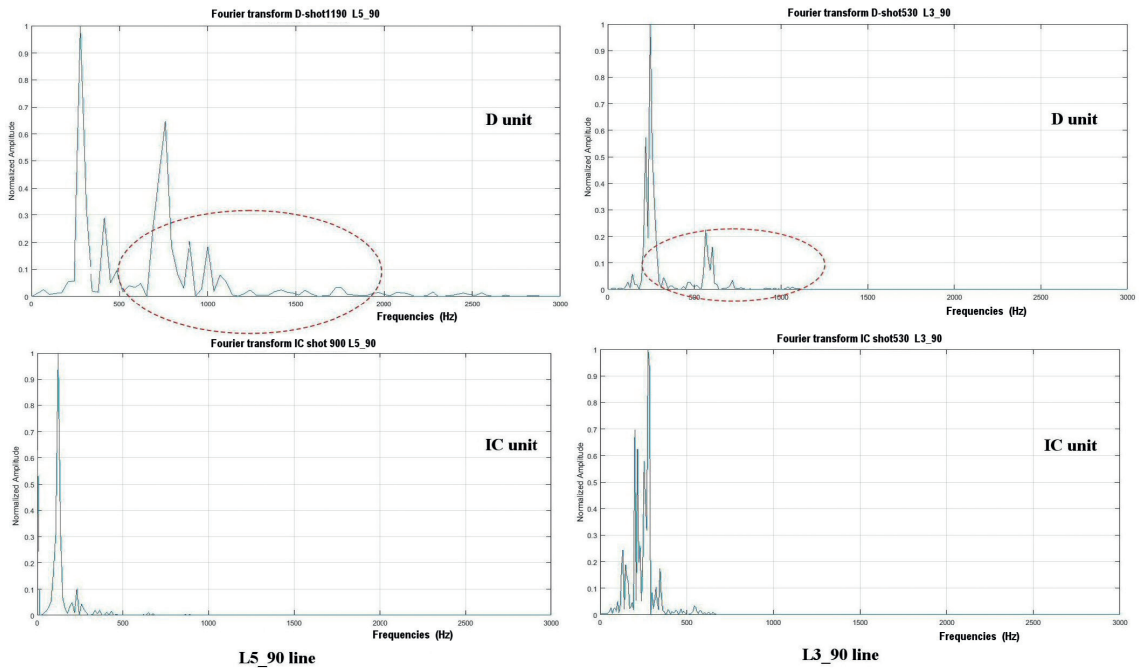
Fig. 17 - FFT of the thicknesses extracted from the seismic lines for both the D unit (upper panel) and IC unit (lower panel).

Table 5 shows the correlation between the data of the two units considered. From the data it is clear that there is no correlation between the IC unit present in the L5_90 line and the D unit of the same line, as highlighted by the scatter-plot in Figs. 18a and 18b. All this is confirmed by the values of correlation coefficient ρ (4th column in Table 5), where it is almost low. The same applies to the IC unit present in the L3_90 line, compared to the D units of the L3_90 and L5_90, where, in fact, ρ is very small, and the results appear completely independent.

Table 5 - Values of cross-correlations carried out between the segments extracted from the seismic lines.

Unit		Unit	Corr. coeff. (*ρ*)
IC L5_90	vs	D L5_90	0.0018
IC L5_90	vs	D L3_90	0.0290
IC L3_90	vs	D L3_90	0.0530
IC L3_90	vs	D L5_90	0.0021
IC L3_90	vs	IC L5_90	0.5200
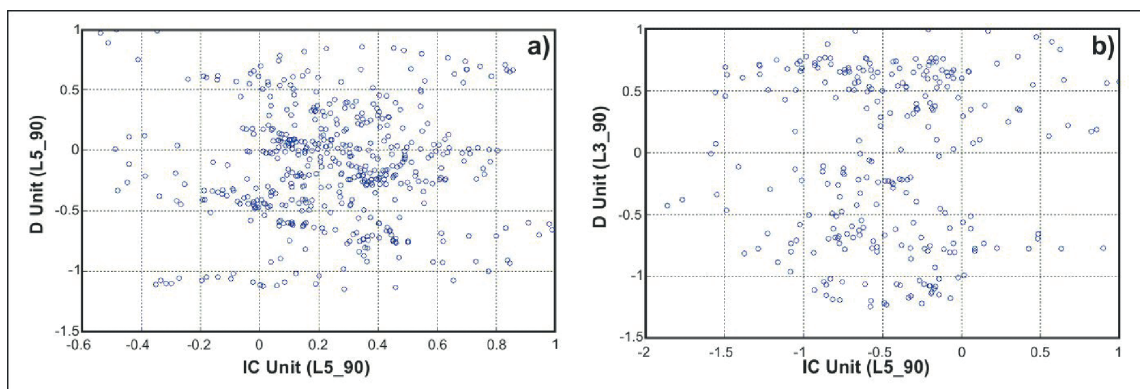
Fig. 18 - Scatter plot of the D unit: a) L5_90 versus the IC unit of line L5_90; b) L3_90 versus the IC unit of line L5_90.

Table 5 shows the correlation between the data of the two units considered. From the data it is clear that there is no correlation between the IC unit present in the L5_90 line and the D unit of the same line, as highlighted by the scatter-plot in Figs. 18a and 18b. All this is confirmed by the values of correlation coefficient ρ (4th column in Table 5), where it is almost low. The same applies to the IC unit present in the L3_90 line, compared to the D units of the L3_90 and L5_90, where, in fact, ρ is very small, and the results appear completely independent.

The comparison between the IC unit of line L3_90 and the IC unit of line L5_90 shows a correlation coefficient, ρ, with high values (highlighted in red in the last line of Table 5), thus, confirming the strong similarity between the characters of the two units, even if present in different lines.

Fig. 19 shows the strong correlation between the IC unit of line L3_90 and the IC unit of line L5_90, as can be seen from the high value of the goodness coefficient R^2 = 0.7987 at the top of the figure.
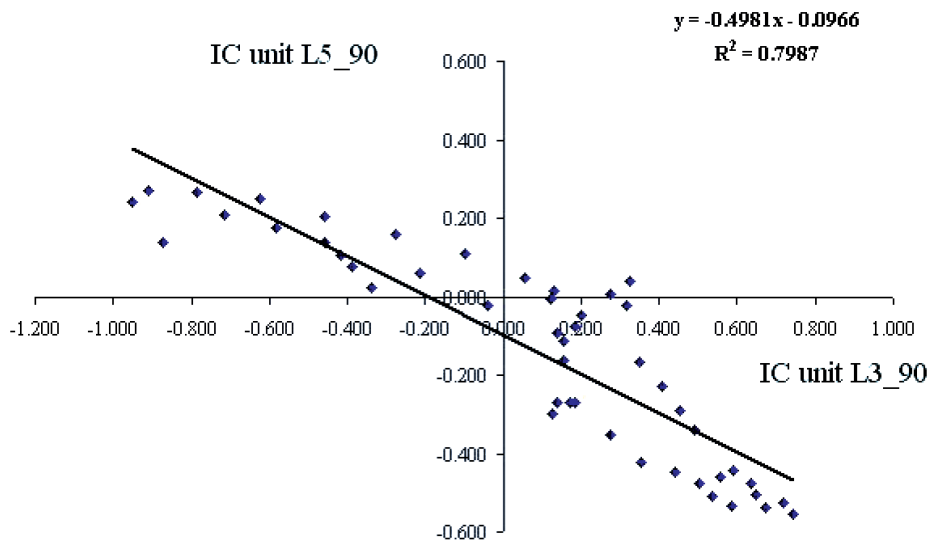
Fig. 19 - Scatter plot between IC unit of L3_90 and IC unit of L5_90.

5. Conclusions

In this work we demonstrate that the spectral signature, FFT2, can be used for stratigraphic differentiation in the recognition of geologic units on single-channel seismic lines. The results clearly show (Fig. 2) the discrimination of the two seismic units, IC and D, identified on the seismic lines, defined Campanian ignimbrite (39 kyr B.P.) and Holocene marine sediments (post 39 kyr B.P.), respectively (Milia *et al.*, 1998a).

The FFT2 confirms that the two units present different specific signatures related to different sedimentological contents as shown in Figs. 7 to 9. The observation of the ROI sample of the IC unit, relating to the Campanian ignimbrite deposit, presents a *R* matrix characterised by low variability, almost homogeneous to the eye, with a frequency content tending towards low. The D unit sample presents a *R* matrix with variable characteristics; it is irregular and stratified, with the amplitude spectrum distributed along the horizontal plane, with a spectral content towards high frequencies (Fig. 11).

Table 2 shows the zero-crossing and variance values of the signals extracted from the shots (layers), relating to the IC and D units. The comparison of the data provided a very significant result, in particular for the statistical index variance. The response of the zero-crossing index is not very satisfactory (as it is related to the length of the signal extracted from the shot which, in turn, coincides with the identified thickness). However, it should still be taken into consideration, as its values present a slight similarity between the two lines. For unit IC the variance appears on average with very low values compared to the results obtained for unit D, as can be seen from the data in Table 2.

The confirmation of the results obtained in Table 2 is shown in Fig. 16, where the data distribution trend and the related histograms of the IC unit and D unit are represented for the

two sample lines examined. The D unit presents itself with linear stratifications as they appear on the seismic lines, characterised by a high variance value, while the IC unit, which appears chaotic and homogeneous, is certainly characterised by a low variance value.

The values of the correlation coefficients determined for the two units are reported in Table 5. A robust correlation and a strong linearity between the IC unit of the L3_90 line and the IC unit of the L5_90 line is noted. In fact, this is confirmed by the high value of correlation coefficient ρ, which confirms the similarity between the units.

Considering Fig. 17, it can be stated that this method confirms the presence of the frequency components evaluated during the FFT of the individual shots. In fact, it is confirmed that the IC unit is oriented towards low frequencies, in particular it is involved in a range of frequencies that varies in band (from 200 to 500 Hz), while the D unit is characterised by much higher frequencies (Fig. 11).

A final data point of particular importance is the measurement of R, which, as already mentioned, characterises the materials from the point of view of hardness (Table 4). In fact, the IC unit, being a compact material compared to the surface sediments (D unit), presents high values of R. The use of the Seismic CLASS toolbox made it possible to provide a geophysical reference for the unambiguous recognition of two important very abundant seismic units in the Gulf of Naples, where, up to present, they were only correlated with terrestrial and marine geognostic wells.

Ultimately, the result of the signature of the FFT2, applied to samples extracted from the areas of interest, can be defined a good indicator for the discrimination of geological units.

The applied method appears efficient in its operation although from the point of view of reliability it is strictly linked to the quantity of signatures that can be stored by creating a real library, in order to continuously compare the acquired data. Therefore, this method can be used to create a database of signatures (geological units), and, then, apply before and/or after geophysical interpretation on seismic lines to obtain a correct interpretation and identification of units, with no doubts. As mentioned above, however, the method can lead to ambiguity in the response in cases where seismic reflector reversals or deflections occur, so we plan not to apply this method to avoid incorrect interpretations.

REFERENCES

Acocella V. and Funiciello R.; 1999: *The interaction between regional and local tectonics during resurgent doming: the case of the island of Ischia, Italy.* J. Volcanol. Geotherm. Res., 88, 109-123, doi: 10.1016/S0377-0273(98)00109-7.

Acocella V. and Funiciello R.; 2006: *Transverse systems along the extensional Tyrrhenian margin of central Italy and their influence on volcanism.* Tectonics, 25, doi: 10.1029/2005TC001845.

Acocella V., Funiciello R., Marotta E., Orsi G. and De Vita S.; 2004: *The role of extensional structures on experimental calderas and resurgence.* J. Volcanol. Geotherm. Res., 129, 199-217, doi: 10.1016/S0377-0273(03)00240-3.

Aiello G., Budillon F., Cristofalo G., D'Argenio B., de Alteriis G., De Lauro M., Ferraro L., Marsella E., Pelosi N., Sacchi M. and Tonielli R.; 2001: *Marine geology and morphobathymetry in the bay of Naples, (south-eastern Tyrrhenian sea, Italy)*. In: Faranda F.M., Guglielmo L. and Spezie G. (eds), Mediterranean Ecosystems, Springer Verlag, Berlin, Germany, pp. 1-8, doi: 10.1007/978-88-470-2105-1_1.

Aiello G., Angelino A., D'Argenio B., Marsella E., Pelosi N., Ruggieri S. and Siniscalchi A.; 2005: *Buried volcanic structures in the Gulf of Naples (southern Tyrrhenian Sea, Italy) resulting from high resolution magnetic survey and seismic profiling.* Ann. Geophys., 48, 1-15, doi: 10.4401/ag-3241.

Aiello G., Barra D., De Pippo T., Donadio C. and Petrosino C.; 2007: *Geomorphological evolution of Phlegrean volcanic islands near Naples, southern Italy.* Z. Geomorph., 51, 165-190, doi: 10.1127/0372-8854/2007/0051-0165.

Baddeley R.; 1997: *The correlational structure of natural images and the calibration of spatial representations.* Cognitive Sci., 21, 351-372, doi: 10.1207/s15516709cog2103_4.

Bellucci F.; 1998: *Nuove conoscenze stratigrafiche sui depositi effusivi ed esplosivi nel sottosuolo dell'area del Somma-Vesuvio.* Boll. Soc. Geol. It., 117, 1-21.

Brocchini D., Principe C., Castratori D., Laurenzi M.A. and Gorla L.; 2001: *Quaternary evolution of the southern sector of the Campanian plain and early Somma-Vesuvio activity: insights from Trecase1 well.* Mineral. Petrol., 73, 67-91, doi: 10.1007/s100170011.

Buogo S. and Cannelli G.B.; 1999: *Source level and directivity pattern of an underwater pulsed sound generator based on electrical discharge.* Acoust. Lett., 23, 54-59.

D'Argenio B., Aiello G., de Alteriis G., Milia A., Sacchi M., Tonielli R., Angelino A., Budillon F., Chiocci F.L. and Conforti A.; 2004: *Digital Elevation Model of the Naples Bay and adjacent area (eastern Tyrrhenian Sea, Italy).* Atlante di Cartografia Geologica, "Mapping Geology in Italy", APAT, Rome, Italy.

De Dominicis Rotondi A.; 1990: *Principi di elettroacustica subacquea, vol. 1.* ED. A.I., 397 pp., ISBN: 97888251116.

De Vivo B., Rolandi G. and Gans P.; 2001: *New constraints on the pyroclastic eruptive history of the Campanian volcanic plain (Italy).* Mineralogy and Petrology, 73, 47–65, doi: 10.1007/s007100170010.

Fakiris E. and Papatheodorou G.; 2012: *Quantification of regions of interest in swath sonar backscatter images using grey-level and shape geometry descriptors: the TargAn software.* Mar. Geophys. Res., 33, 169-183, doi: 10.1007/s11001-012-9153-5.

Farinella G.M., Ravìa D., Tomaselli V., Guarnera M. and Battiato S.; 2015*: Representing scenes forreal-time context classification on mobiledevices*. Pattern Recognit., 48, 1086-1100, doi: 10.1016/j.patcog.2014.05.014.

Giordano A. and Giordano L.; 2012: *Osservazione del comportamento della colonna d'acqua rispetto ai segnali Sparker nel mare antartico.* In: Atti della Fondazione Giorgio Ronchi, Firenze, Italy, Anno LXVII, n. 5, pp. 654-673.

Giordano A., De Luca L., De Luca C., Giordano P. and Giordano L.; 2015: *Controllo del guadagno in ampiezza di segnali sismici a riflessione nel dominio del tempo mediante il filtro TVG (Time Varying Gain).* In: Atti della Fondazione Giorgio Ronchi, Firenze, Italy, Anno LXX, n. 2, pp. 215-225.

Ippolito F., Ortolani F. and Russo M.; 1973: *Struttura marginale tirrenica dell'Appennino campano: reinterpretazioni di dati di antiche ricerche di idrocarburi.* Mem. Soc. Geol. It., 12, 227-250.

Jones E.J.W.; 1999: *Marine geophysics*. J. Wiley & Sons, Hoboken, NJ, USA,, 474 pp., ISBN: 978-0-471-98694-2.

McQuillin R., Bacon M. and Barclay W.; 1979: *An Introduction to seismic interpretation.* Graham & Trotman Ltd, London, UK, 224 pp., ISBN: 0860101118.

Milia A.; 1998: *Le unità piroclastiche tardo-quaternarie nel Golfo di Napoli.* Geogr. Fis. Dinam. Quat., 21, 147-153.

Milia A.; 1999: *The geomorphology of Naples bay continental shelf (Italy).* Geogr. Fis. Dinam. Quat., 22, 73-78.

Milia A.; 2000: *The Dohrn canyon: a response to the eustatic fall and tectonic uplift of the outershelf along the eastern Tyrrenian sea margin, Italy.* Geo-Mar. Lett., 20, 101-108, doi: 10.1007/s003670000044.

Milia A. and Torrente M.M.; 1997: *Evoluzione tettonica della Penisola Sorrentina (margine peritirrenico campano).* Boll. Soc. Geol. It., 116, 487-502.

Milia A. and Torrente M.; 1999: *Tectonics and stratigraphic architecture of a peri-Tyrrhenian halfgraben (bay of Naples, Italy).* Tectonophys., 315, 301-318, doi: 10.1016s0040-1951(99)00280-2.

Milia A. and Torrente M.; 2003: *Late Quaternary volcanism and transtensional tectonics in the Naples Bay, Campanian continental margin, Italy.* Mineral. Petrol., 79, 49-65, doi: 10.1007/s00710-003-0001-9.

Milia A. and Torrente M.M.; 2011: *The possible role of extensional faults in localizing magmatic activity: a crustal model for the Campanian volcanic zone (eastern Tyrrhenian Sea, Italy).* J. Geol. Soc., 168, 471–484, doi: 10.1144/0016-76492010-121.

Milia A., Mirabile l., Torrente M. and Dvorak J.J., 1998a: *Volcanism offshore of Vesuvius in Naples Bay.* Bull. Volcanol., 59, 404-413.

Milia A., Torrente M.M. and Nardi G.; 1998b: *Recent tectonic and magmatic features off the coast of Naples.* Giornale di Geologia, 60, 27-39.

Milia A., Torrente M., Russo M. and Zuppetta A.; 2003: *The Tectonics and crustal structure of the Campanian continental margin: relationships with volcanism*. Mineral. Petrol., 79, 33-47, doi: 10.1007/s00710-003-0005-5.

Mirabile L., Fevola F., Galeotti F., Ranieri G. and Tangaro G.; 1991: *Sismica monocanale ad alta risoluzione con sorgente multispot di tipo Sparker: applicazione ai dati di tecniche di deconvoluzione.* In: Atti 10° Conv. Ann. Gruppo Nazionale di Geofisica della Terra Solida, Esagrafica, Roma, pp. 431-444.

Oliva A. and Torralba A.; 2001: *Modeling the shape of the scene: a holistic representation of the spatial envelope.* Int. J. Comput. Vision, 42, 145-175.

Oliva A. and Torralba A.; 2002: *Depth estimation from image structure.* IEEE Transactions on pattern analysis machine intelligence, 24, doi: 10.1109/TPAMI.2002.1033214.

Oliva A., Torralba A., Guerin-Dugue A. and Herault J.; 1999: *Global semantic classification of scenes using power spectrum templates.* In: Challenge of Image Retrieval (CIR99), Newcastle upon Tyne, UK, 11 pp., doi: 10.14236/ewic/CIR1999.9.

Robinson E.A: 1984: *Seismic inversion and deconvolution. Part A: classical methods.* Handbook of Geophysical Exploration, 4, Pergamon, Champaign, IL, USA, 349 pp., ISBN: 0946631042.

Roca M.; 2015: *Evoluzione stratigrafica, sedimentologica e geomorfologica durante il quaternario di un settore di margine tirrenico campano: Il Canyon Dohrn nel golfo di Napoli (Tirreno Meridionale)*. Corso di Dott. in: Scienze del Mare della Terra e del Clima, XXVII Ciclo, Università degli Studi di Napoli Parthenope, Napoli, Italy, **?? pp.**

Rolandi G. and Bellucci F.; 2003: *Attività interpliniane del Somma negli ultimi 3700 anni ed evoluzione calderica dell'edificio.* Riassunti Workshop Vesuvio: dentro il vulcano, Ercolano, 8-10 maggio 2003.

Rosi M. and Sbrana A. (eds); 1987: *Phlegraean Fields.* Quaderni de La Ricerca Scientifica, 114, Consiglio Nazionale delle Ricerche, Roma, 175 pp.

Simpkin P.G.; 2005: *The Boomer sound source as a tool for shallow water geophysical exploration.* Mar. Geophys. Res., 26, 171-181, doi: 10.1007/s11001-005-3716-7.

Torralba A. and Oliva A.; 2003: *Statistics of natural image categories.* Institute of Physics Publishing, Network: Comput. Neural Syst., 14, 391-412, PII: S0954-898X (03)53778-2.

Urick R.J.; 1979: *Sound propagation in the sea.* U.S. Gov. Print. Off., Washington, USA, 250 pp.

Van der Schaaf A. and van Hateren J.H.; 1996: *Modeling of the power spectra of natural images: statistics and information*. Vision Res., 36, 2759-2770, doi: 10.1016/0042-6989(96)00002-8.

Corresponding author: Alberto Giordano
                                            Seconda Università degli Studi di Napoli "Parthenope"
                                            Centro Direzionale Isola C4, 80133 Napoli, Italy
                                            Phone: +39 081 5476668; e-mail: alberto.giordano@uniparthenope.it